Tuning the Optical Band Gap of Quantum Dot Assemblies by Varying Network Density

ARTICLE *in* ACS NANO · AUGUST 2009

Impact Factor: 12.88 · DOI: 10.1021/nn900456f · Source: PubMed

3 AUTHORS, INCLUDING:

Hongtao Yu
Jackson State University
96 PUBLICATIONS **2,784** CITATIONS
SEE PROFILE

Stephanie Brock
Wayne State University
124 PUBLICATIONS **3,039** CITATIONS
SEE PROFILE

ARTICLE

Tuning the Optical Band Gap of Quantum Dot Assemblies by Varying Network Density

Hongtao Yu, Yi Liu, and Stephanie L. Brock*

Department of Chemistry, Wayne State University, Detroit, Michigan 48202

ABSTRACT The effect of bulk network density on the extent of quantum confinement (probed by optical band gap) in CdSe quantum dot gels is evaluated. The CdSe gels were produced from controlled removal of surface thiolate ligands from CdSe quantum dots by adding 3% tetranitromethane. Two main techniques were employed to systematically vary the bulk density. First, different amounts of oxidizing agent were added to change the monolith density of the wet gel, followed by supercritical CO_2 drying to yield CdSe aerogels with different bulk densities. Experimental results suggest that a gradual and almost linear band gap decrease is observed when increasing the bulk density at the aerogel level. The fact that quantum confinement effects are largely preserved in aerogel constructs is consistent with SAXS data revealing the fractal nature of the network. Second, for a constant amount of oxidant, different drying techniques were used to yield CdSe gels with a larger density variation: aerogels (supercritical CO_2 dried), ambigels (hexane dried), and xerogels (acetone dried). A nonlinear trend for band gap decrease was found when comparing CdSe aerogels, ambigels, and xerogels, and the more dense ambi- and xerogels have broader absorption edges, suggestive of resonance transfer effects due to dipole—dipole interactions in non-homogeneous interacting systems. This is attributed to increased aggregation in the denser constructs (supported by TEM and SAXS data). Together, these data suggest that highly porous architectures, such as aerogels, are best suited for maintaining localized quantum confinement effects in 3D connected nanoparticle networks.

KEYWORDS: CdSe · quantum dots · chalcogenide gels · density · dimensionality · quantum confinement · aerogel · xerogel

The effect of dimensionality on a material's electronic and optical properties is a hot topic in the study of nanomaterials. Experimental and theoretical studies have shown that the band gap evolution observed in InP 2D-confined nanowires is weaker than that of InP 3D-confined nanodots, due to the loss of one confinement dimension.[1] Additionally, studies of CdSe nanorods with intermediate dimensions between 0 and 1 have demonstrated that tuning the diameter of nanorods can more effectively vary the band gap absorption and photoluminescence energy than tuning the length of CdSe nanorods.[2] Recently, our lab has developed a general methodology to assemble semiconducting nanoparticles into a low dimensional and fractal gel network *via* oxidative decomplexation of thiolate-capped CdSe quantum dots (QDs).[3,4] Depending on how the wet gels are dried, the density can be systematically varied. Drying from supercritical carbon dioxide is most effective for preserving the wet gel structure, yielding an aerogel. On the other hand, drying under ambient conditions from the mother liquor (a surface wetting solvent) results in significant compaction due to capillary forces acting on the pores during solvent evaporation, yielding a xerogel. Thus, this assembly technique naturally offers a platform to evaluate how bulk density and dimensionality impact quantum confinement effects in fractal networks. Previous work in our lab demonstrated that xerogels prepared from metal chalcogenide nanoparticles (PbS, CdSe, CdS, and ZnS) exhibit intermediate optical band edges between the corresponding bulk materials and the more porous aerogel counterparts,[5] whereas those made from CdSe@ZnS core/shell nanoparticles remain perfectly quantum confined (*i.e.*, the band gap is the same regardless of the composite density).[6] These data suggest that the local dimensionality of the network governs the extent of interaction in such systems. Where this value is constrained to zero by the presence of a ZnS shell, there is no density dependence, whereas in "naked" nanoparticle network systems, the extent of quantum confinement is directly related to the density and characteristic pore structure.

In the present contribution, we systematically evaluate how bulk density and dimensionality influence quantum confinement in gel frameworks composed from CdSe quantum dots. CdSe was chosen be-

*Address correspondence to sbrock@chem.wayne.edu.

Received for review May 5, 2009 and accepted June 24, 2009.

Published online July 2, 2009.
10.1021/nn900456f CCC: $40.75

cause it represents a well-developed system in terms of straightforward synthesis and the ability to control particle size precisely, resulting in sharp absorption onsets for evaluation of quantum confinement.[7,8] In order to rationally vary the density and dimensionality of the gel network, two approaches were used. First, different quantities of gelation agent were added to vary the monolith density of the wet gel, followed by supercritical CO_2 drying to yield aerogels (lowest density monoliths). Second, for a constant amount of oxidant, different drying techniques were employed to vary the density of the network over a larger scale, thus creating ambigels (intermediate density monoliths prepared by drying from a nonwetting solvent) and xerogels (highest density monoliths).

RESULTS AND DISCUSSION

CdSe quantum dots with a narrow size distribution (9.4%) were synthesized *via* a modification of a typical colloidal method that employed high boiling point coordinating solvents.[7−9] Thiolate ligand exchange on the quantum dot surface followed by oxidant addition leads to gelation by oxidative removal of thiolate ligands and consequent formation of interparticle bonds.[1,3,4,10,11] The degree of interconnectivity among CdSe dots was varied by adding a series of amounts (2.5, 5, 10, 15, and 20 μL) of the gelation agent (3% tetranitromethane, TNM) into concentration identical CdSe dot sols (in methanol). The wet gels were aged for 1 week in the mother liquor, solvent-exchanged with acetone to remove the disulfide byproducts,[12,13] and then subjected to supercritical CO_2 drying to yield aerogels of varying density, based on the amount of oxidant used.[14,15] Alternatively, drying of wet gels (prepared from 20 μL of TNM) under ambient conditions from hexane (a nonwetting solvent) or acetone (a wetting solvent) yielded more dense ambigels and xerogels,[15] respectively, due to capillary forces (moderated by the extent of solvent wetting) as the solvent evaporates from the pores. The bulk densities of the gel networks were determined by dividing the mass of the monolith CdSe dried gels over the physical gel volume (aerogel density = 0.006−0.033 g/cm^3, ambigel density = 0.18 g/cm^3, xerogel density = 0.20 g/cm^3).

The crystalline phase, structure, and morphology of CdSe quantum dots and the resultant aerogels, ambigels, and xerogels were evaluated by powder X-ray diffraction (PXRD) analysis and transmission electron microscopy (TEM). The PXRD patterns (Figure 1) demonstrate that the hexagonal crystalline phase observed in the primary CdSe nanoparticles is retained upon gelation, similar to our previous observations.[10,16,17] The almost-identical peak shapes indicate that, upon the gelation and drying process, the primary CdSe nanocrystals (average diameter = 3.37 nm, measured by a modified Scherrer equation[18]) are connected into a 3D gel framework without significant crystallite grain

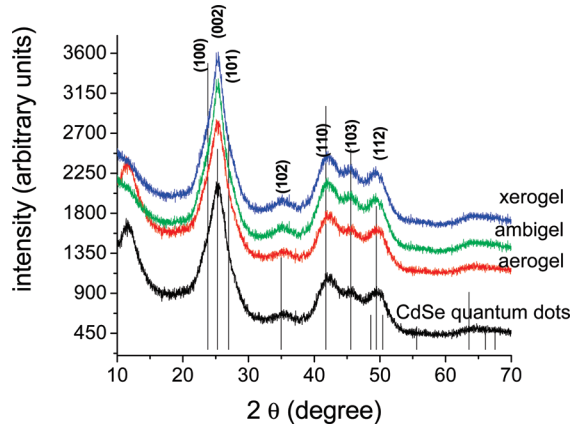

Figure 1. X-ray diffraction patterns of CdSe quantum dots and the resultant aerogel, ambigel, and xerogel. The vertical lines are from PDF file #08-0459 (hexagonal CdSe).

growth, regardless of the different types of drying techniques.

In contrast, the drying technique does have a significant impact on the general morphology of the resultant CdSe dried gels. When monodisperse CdSe quantum dots (3.17 ± 0.31 nm by TEM) were assembled into a gel network *via* oxidative gelation, varying the amounts of the oxidizing agent seemed to have little influence on the general morphology of the CdSe aerogels produced by supercritical drying. All aerogels exhibit a characteristic pearl necklace morphology similar to base-catalyzed silica aerogels (Figure 2A),[19] with easily identifiable open pores of a range of sizes. However, pores are difficult to discern in the TEM images of samples of CdSe ambigels and xerogels; instead, large aggregates composed of CdSe primary particles are observed (Figure 2B,C). This confirms the expectation that conventional drying methods cause a significant collapse of the wet gel structure and pore closure relative to supercritical CO_2 drying. Thus, the morphology

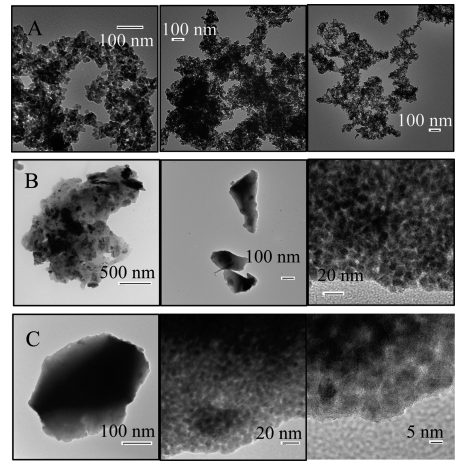

Figure 2. Transmission electron micrographs at different magnifications of (A) CdSe quantum dot aerogels, (B) ambigels, and (C) xerogels. The presence of densely packed CdSe primary building blocks in ambigels and xerogels can be clearly seen in the high-magnification TEM images (B,C; far right).

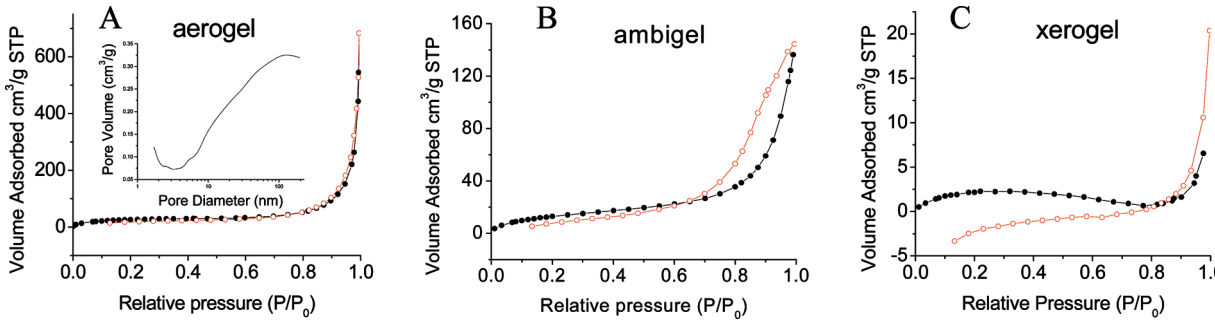

Figure 3. Nitrogen adsorption (black filled circles)/desorption (red empty circles) isotherms for CdSe quantum dot gels: (A) aerogel (inset is BJH pore size distribution), (B) ambigel, (C) xerogel. The drop in the desorption isotherm below that of the adsorption isotherm is attributed to outgassing of helium entrapped in micropores during free-space measurements preceding isotherm collection. It is more pronounced in low-surface area materials (*i.e.*, ambigel and xerogel).[20]

of the CdSe ambigel is closer to that of the xerogel than it is to the aerogel.

Surface area and porosimetry data on CdSe gels were obtained by analysis of nitrogen adsorption/desorption isotherms. The isotherms of a representative aerogel, ambigel, and xerogel are all shown in Figure 3, and the shape of isotherm curves is consistent with a mesoporous type of material.[20,21] The Brunauer−Emmett−Teller (BET) surface areas based on monolayer N_2 gas coverage for the series of CdSe aerogels with different bulk densities yield similar values: 98−118 m^2/g (Supporting Information, Table S1), and there is no direct relationship between aerogel surface areas and corresponding bulk densities. However, consistent with the visual observation of increasing bulk densities, comparison of the BET surface areas of the CdSe aerogel, ambigel, and xerogel shows that the aerogel exhibits the highest surface areas (100 m^2/g), while the xerogel has the lowest value (9 m^2/g) and the ambigel is intermediate (52 m^2/g).

To investigate the effect of density on quantum confinement in 3D CdSe gel networks, we employed diffuse reflectance UV/visible/NIR spectroscopy techniques for CdSe gel band gap measurements. Spectra collected from a series of CdSe aerogels with different bulk densities are shown in Figure 4A. The onsets of the curves are generally sharp, similar to data on discrete CdSe particles. Compared with the onset value of primary particles (2.150 eV), the band gaps of CdSe aerogels exhibit a slight red shift. Moreover, a gradual but discernible band gap decrease for CdSe aerogels was observed when different volumes of 3% tetranitromethane were added into CdSe nanoparticle sols to yield different-volume monoliths (Figure 4B). The nearly linear decrease in band gap with increasing density suggests that the degree of quantum confinement in CdSe aerogel networks is a direct function of their bulk density.

In contrast, as shown in Figure 5, relatively large changes in band gap are observed when different drying techniques are used. The band gap difference between CdSe aerogels (close to that of the primary particles, 2.15 eV) and xerogels (close to that of the bulk semiconductor, 1.74 eV) has been previously noted in metal chalcogenide gels.[5] The inclusion of data from the ambigel reveals a more complex relationship between density and band gap than observed in the aerogel series alone, suggesting other contributing effects. These are likely to include resonance transfer due to dipole−dipole interactions between different sizes of quantum confined units. Presumably, these arise in the ambi- and xerogel due to aggregation, creating an inhomogeneous distribution of chromophore sizes even as the native crystallite sizes are uneffected. Dipole−dipole interactions also explain the increased

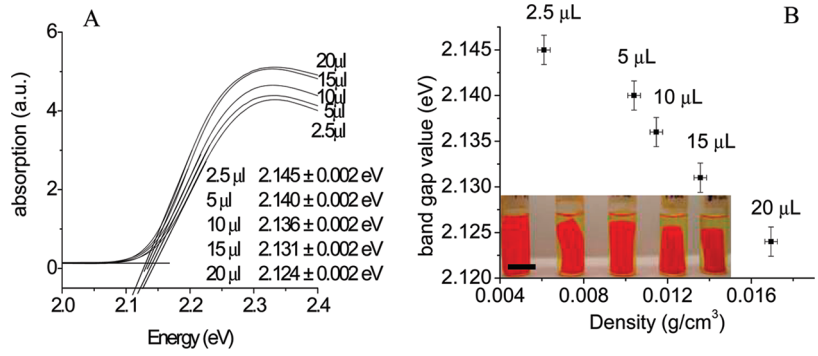

Figure 4. (A) Absorbance plots for a series of CdSe aerogels prepared with different volumes of 3% tetranitromethane. (B) Plot of aerogel band gap *vs* monolith density. The inset shows corresponding images of wet gels (2.5 to 20 µL tetranitromethane, left to right); scale bar = 1 cm.

broadening in the absorption onset of ambigels and xerogels relative to aerogels (Figure 5A).[22]

Small-angle X-ray scattering (SAXS) was employed to discern whether there is a relationship between the mass and surface fractal dimensionality of CdSe gels and their corresponding bulk densities. However, the CdSe quantum dot aerogels were found to have essentially identical scattering curves (intensity *vs* 2θ, Supporting Information, Figure S1) regardless of the monolith density (amount of oxidant added). In contrast, the scattering curves for ambigel and xerogel are quite distinct from those of the aerogel, as shown in Figure 6.

Quantitative analysis of the scattering provides information on the surface and mass fractal characteristics of the gels. The scattering intensity, $I(Q)$, can be described as $I(Q) \sim F(Q)S(Q)$, where $F(Q)$ is the form factor, which is related to the size and shape of the particles, and $S(Q)$ is the structure factor, which describes the correlation between particles.[23] Q is the scattering factor and is related to the scattering angle, θ, by $Q = (4\pi/\lambda)\sin(\theta/2)$, where λ is the wavelength of X-ray radiation. For mass fractal aggregates, the scattered intensity is mainly dominated by the structure factor $S(Q)$, while for surface fractals, the scattered intensity is dictated predominantly by the form factor $F(Q)$.[24] Thus, for mass fractal aggregates, $I(Q) \approx S(Q) \approx Q^{-D_m}$, where D_m is the mass fractal dimension, and for surface fractals, $I(Q) \approx F(Q) \approx Q^{-(6-D_s)}$, where D_s is the surface fractal dimension.[24] Consequently, the slope of a log−log plot of $I(Q)$ *versus* Q can be used to determine values for D_m and D_s.

Figure 7 shows the scattered intensity *versus* scattering vector Q on a log−log scale. In the mass fractal regime, D_m can be obtained directly from the slope, while in the surface fractal regime, the slope $= -(6 - D_s)$. As shown in Figure 7, the curve for the aerogel reveals two linear slopes that can be reasonably assigned to a mass fractal dimensionality (D_m) of 2.3 and a surface fractal dimensionality (D_s) of 2.8.[23] These data suggest that the CdSe aerogels can be treated as fractal objects with mass dimensionalities intermediate between 2 and 3 (similar to values obtained from silica colloidal aerogels, $D_m \sim 2.4$[25]), but rough surfaces ($D_s = 2.0$ for a smooth surface;[24,26] $D_s = 2.2$ for a colloidal silica aerogel[25]). Moreover, the variation in density (obtained by varying the concentration of oxidant) does not have a discernible effect on the fractal characteristics of the aerogel. The log intensity−log Q curves of CdSe ambigels and xerogels exhibit similarly rough surface characteristics to aerogels ($D_s = 3.0$) but, intriguingly, have no mass fractal characteristics (D_m takes unreasonable values of <1), implying a lack of self-similarity over the length scale probed in the experiment.[27] Thus, the CdSe aerogels are all fractals of similar dimension regardless of monolith density, whereas the more dense ambi- and xerogels are not fractal objects at all.

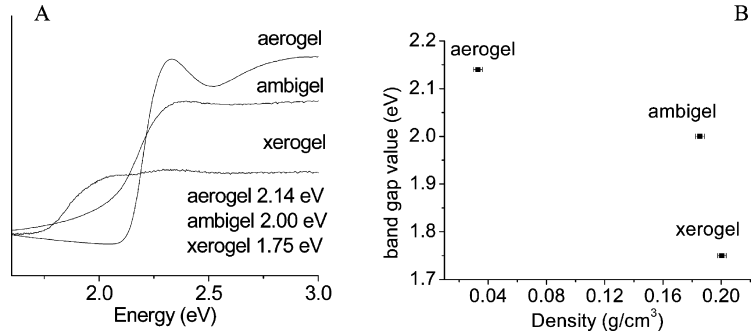

Figure 5. (A) Absorbance plot of CdSe aerogel, ambigel, and xerogel (20 μL 3% TNM for gelation). (B) Plot of band gap *vs* monolith density of CdSe aerogels, ambigels, and xerogels.

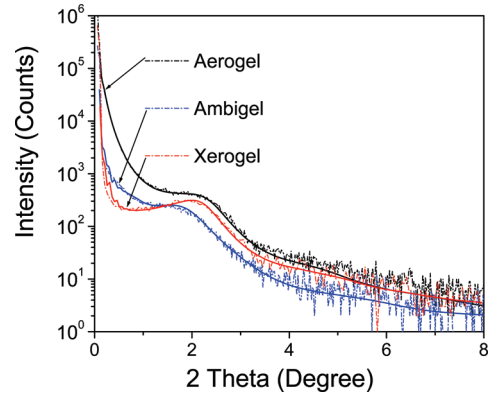

Figure 6. SAXS data (scattering intensity as a function of 2θ) of CdSe aerogel, ambigel, and xerogel prepared with 20 μL of 3% TNM, along with their computer simulation curves (solid lines).

In addition to obtaining information on fractal characteristics, by using standard theory describing the scattered intensity *versus* form factor and structure factor,[24] information on particle/pore size distributions within the different types of gels can be obtained. Figure 8 shows the results of a data simulation, assuming a

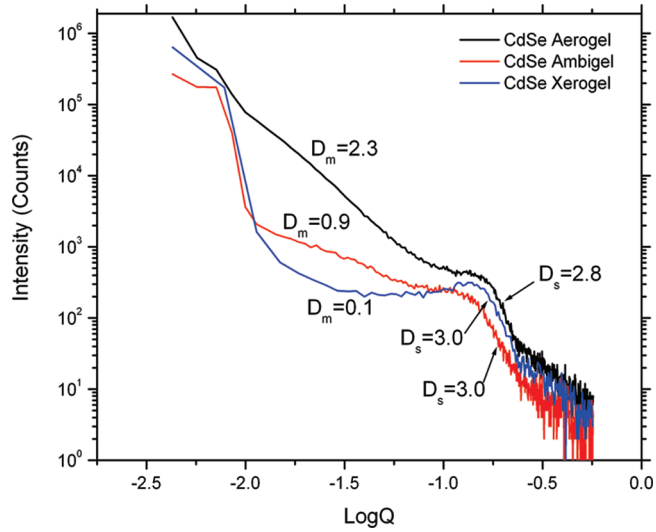

Figure 7. Scattered intensity *versus* scattering vector for the CdSe aerogel, ambigel, and xerogel. The slopes of each curve give information about the dimension of the fractal.

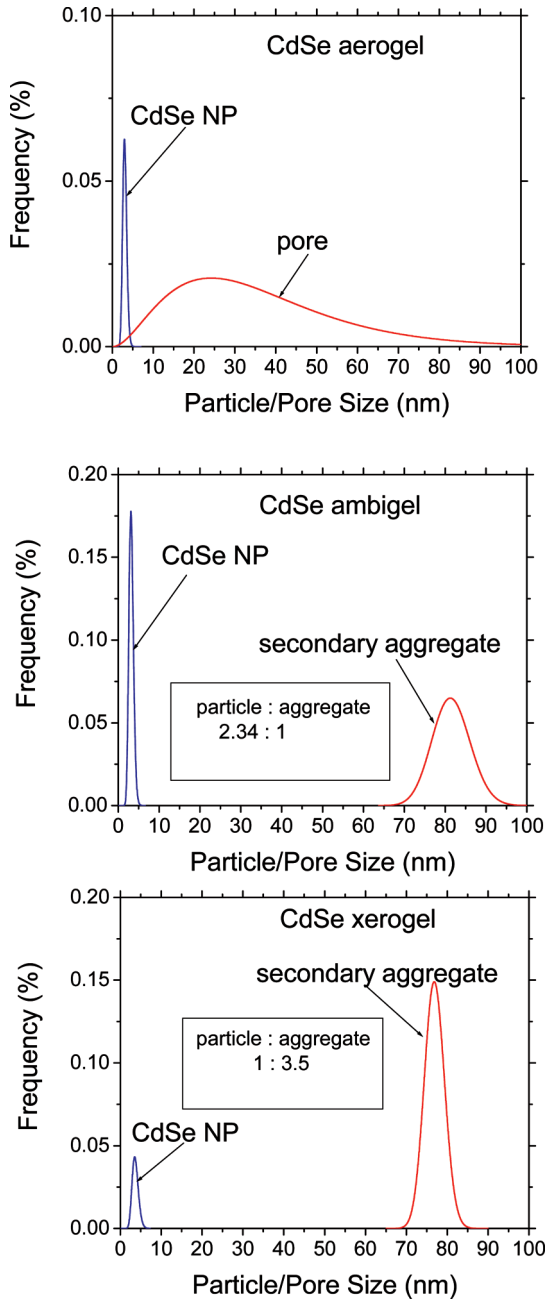

Figure 8. Particle and pore distribution simulation plots for CdSe aerogel, ambigel, and xerogel.

two-phase system composed of particles and pores and/or aggregates. The data could be modeled assuming two distributions. In all cases, the first peak is at *ca.* 3 nm, and this distribution can be assigned to the primary CdSe building blocks based on TEM and XRD size determination (3.17 and 3.37 nm, respectively). The secondary broad distribution in the aerogel plot centered at *ca.* 30 nm is consistent with the breadth and average pore size determined by Barrett–Joyner–Halenda (BJH) modeling of the nitrogen physisorption data (Figure 3A inset and Supporting Information). However, the relatively narrow secondary peaks near 80 nm for the ambigel and xerogel could not be reasonably assigned to pores. Rather, they are more consistent with the presence of large aggregates in the ambigel and xerogel, which is supported by the observations in TEM. On the basis of integrating the two peaks, the extent of aggregation appears to be larger in the xerogel than in the ambigel, as would be expected based on the relative density of the monoliths produced. Overall, the SAXS data (in combination with surface area measurements) suggest that the characteristic porosity of the aerogel (preserved from the wet gel) is lost from the ambi- and xerogels.

CONCLUSIONS

The extent of quantum confinement in nanostructures assembled from discrete nanocrystals of CdSe is found to depend on both the fractal characteristics and density of the network. CdSe aerogels can be effectively described as a fractal framework of discrete nanocrystals encompassing a mesoporous network structure and demonstrate quantum confinement effects that vary systematically with their monolith densities. In contrast, CdSe ambigels and aerogels are non-(mass)fractal networks wherein the nanocrystal framework is predominantly interfaced to itself, leading to formation of large aggregates. Thus, the evolution of optical band gap in ambigels and xerogels is not just a function of the density-dictated extent of quantum confinement as in the aerogels but is complicated by contributions from dipole–dipole interactions between particles. Overall, these data suggest that highly porous architectures, such as aerogels, are best suited for maintaining localized quantum confinement effects in 3D connected nanoparticle networks.

METHODS

Synthesis. ***Materials.*** Trioctylphosphine oxide (TOPO, 90%), cadmium oxide (99.99%), selenium powder (99.5%), 11-mercaptoundecanoic acid (MUA, 95%), tetramethylammonium hydroxide pentahydrate (TMAH, 97%), and tetranitromethane were purchased from Aldrich. Trioctylphosphine (TOP, 97%) was purchased from Strem. *N*-Tetradecylphosphonic acid (98%) was purchased from Alfa-Aesar. Toluene, methanol, ethyl acetate, hexane, acetone, and ethyl alcohol were purchased from Fisher. Liquid CO_2 was supplied by Praxair. TOPO was distilled before using; other chemicals were used as received.

Synthesis of Monodisperse CdSe Quantum Dots. The detailed synthesis and isolation procedure for CdSe quantum dots has been previously published.[17] In a typical reaction, 4.0 g (10.3 mmol) of distilled trioctylphosphine oxide, 0.2 g (0.72 mmol) of *n*-tetradecylphosphonic acid, and 0.05 g (0.37 mmol) of CdO powder were mixed under Ar flow. The temperature was gradually increased to 320 °C and maintained for 6–7 h during which time the solution becomes colorless. The temperature was subsequently reduced to 150 °C, and a stock solution containing

0.032 g (0.30 mmol) of Se in 2.5 mL of trioctylphosphine was rapidly injected into the system. The temperature was ramped up to 230 °C in steps of 10 °C/10 min and held at that temperature for 4 h before the temperature was cooled to 70 °C. Then, 5 mL of toluene was injected, and the CdSe particles were precipitated by adding an excess of ethyl alcohol. To purify the particles, the solution was centrifuged and the sediment was redispersed in toluene. After a second precipitation with ethyl alcohol, the sediment was kept for further analysis.

MUA Capping of CdSe Quantum Dots and Gelation. MUA capping was performed as described in the literature.[17] Briefly, CdSe quantum dots were treated with 0.3 g (1.24 mmol) of 11-mercaptoundecanoic acid in 10 mL of methanol adjusted to pH = 10.5−11 with tetramethylammonium hydroxide at 30 °C in a closed Ar environment overnight. The MUA-capped particles were subsequently precipitated with excess ethylacetate, then purified by repeated dispersion in methanol and precipitation with ethyl acetate (two times). The sediment was dispersed in 11 mL of methanol for further analysis. One milliliter of an 11 mL MUA-capped CdSe quantum dot sol in methanol was diluted 100 times to determine the sol concentration by the Beer−Lambert law *via* UV/visible absorption spectroscopy and using the extinction coefficient for a 3.17 nm CdSe quantum dot as determined by Peng's method.[28] On the basis of this analysis, the original sol concentration from which gels were formed was found to be 0.5−1 mol of primary particles per liter. To make a series of wet gels with different bulk densities, a series of different volumes of 3% tetranitromethane (TNM) (2.5, 5, 10, 15, and 20 μL) were added into 2 mL aliquots of the CdSe nanoparticle sol to form the wet gels. After aging for 7 days, aged gels were exchanged with acetone 6−7 times over 3 days to obtain the purified wet gels. Gelation experiments were conducted in parallel to ensure effects from daily variation of the lab environment (*e.g.*, temperature) would be consistent from sample to sample.

CdSe Aerogel, Ambigel, and Xerogel Formation. The formation of CdSe aerogels has been previously reported.[17] In a typical procedure, acetone-exchanged CdSe wet gels were transferred to a SPI-DRY model critical point dryer where they were subsequently washed and immersed in liquid CO_2. The CO_2-exchanged wet gels were then dried under supercritical conditions by raising the drier temperature to 39 °C followed by venting to ambient pressure, yielding CdSe aerogels. CdSe ambigels and xerogels were dried from wet gels prepared from addition of 20 μL of 3% TNM. Ambigels employ a nonpolar solvent, hexane. First, the original wet gel is exchanged with 10 × 3 mL of hexane and then dried at room temperature and atmospheric pressure on the benchtop for 3 days. Xerogels were generated by benchtop drying of the wet gel from the polar exchange solvent, acetone. The gel densities were calculated by measuring the monolithic aerogel, ambigel, and xerogel mass and dividing by the corresponding gel physical volume.

Characterization. ***Powder X-ray Diffraction.*** Powder X-ray diffraction (PXRD) analysis was employed to study the phase and crystallinity of the CdSe quantum dots and resultant gels. A Rigaku RU 200B X-ray diffractometer (40 kV, 150 mW, Cu Kα radiation) with rotating anode was used for X-ray diffraction measurements. Powdered samples of CdSe aerogels, ambigels, and xerogels were deposited on a low background quartz (0001) holder coated with a thin layer of grease. X-ray diffraction patterns were identified by comparison to phases in the International Centre for Diffraction Data (ICDD) powder diffraction file (PDF) database (release 2000).

Transmission Electron Microscopy. Transmission electron microscopy (TEM) was employed to study CdSe quantum dots and the morphology of the resultant gels. The TEM analyses were conducted in the bright field mode using a JEOL FasTEM 2010 HR TEM analytical electron microscope operating at an accelerating voltage of 200 kV. Particle samples were prepared by depositing a drop of a dilute toluene dispersion of CdSe nanocrystals on carbon-coated copper grids and subsequently evaporating the solvent. The average particle size and standard deviation were determined from the measurement of over 1000 particles. Aerogel, ambigel, and xerogel samples were prepared on carbon-coated copper grids by first grinding the solid gel samples to fine powders and then pressing the TEM grid onto the dried powder.

Surface Area Analysis. The surface areas of CdSe aerogels, ambigels, and xerogels were obtained by nitrogen adsorption/desorption isotherms acquired at 77 K on a Micromeritics ASAP 2010 surface area analyzer. Powdered samples were degassed at 100 °C for 48 h prior to the analysis. This heating is expected to result in a small degree of crystallite growth, as was demonstrated in previous studies,[3,29] although band gap and X-ray powder diffraction measurements were not conducted on post-heated samples in this specific case. Data were acquired employing a 30 s equilibrium interval and a 5 cc dose for a total running time of about 7−10 h. The data were fit by using the Brunauer− Emmett−Teller (BET) model to determine the surface areas of the aerogels, ambigels, and xerogels. The average pore diameter and cumulative pore volume for the aerogels were calculated by using the Barrett−Joyner−Halenda (BJH) model based on cylinder pore geometry.

Optical Absorption Measurements. Optical absorption measurements of MUA-capped CdSe quantum dots in methanol were conducted on a Hewlett-Packard (HP) 8453 spectrophotometer. A dilute CdSe nanoparticle suspension was analyzed against a methanol blank in the region from 400 to 700 nm. A Jasco V-570 UV/vis/NIR spectrophotometer equipped with an integrating sphere was used to measure the optical diffuse reflectance of the resultant CdSe gels. Powdered samples of CdSe aerogels, ambigels, and xerogels were evenly spread on a sample holder preloaded with a reflectance standard and measured from 200 to 1500 nm. The band gaps of the samples were estimated from the onset of absorption in data converted from reflectance.[30,31] As the band gaps of aerogels were very similar, data were acquired at 2 nm (0.0016 eV) resolution to precisely differentiate between samples.

Small-Angle X-ray Scattering (SAXS). A Smartlab Rigaku X-ray diffractometer (40 kV, 44 mA, Cu Kα radiation) was employed in transmission mode for SAXS measurements. Finely powdered samples of CdSe aerogels, ambigels, and xerogels were loaded into 0.3 mm boron-rich capillary tubes for measurements, and the intensity of the scattered X-rays was recorded from 0 to 8° 2θ. D_m (mass fractal dimensionality) and D_s (surface fractal dimensionality) measurements were based on slope calculations of log intensity−log Q curves,[25] whereas the particle/pore (or aggregate) size distributions were obtained from computer simulation of the raw data using the software Nano-Solver.[32,33]

Acknowledgment. This work was supported by the National Science Foundation (DMR-0701161) and the donors of the Petroleum Research Fund, administered by the American Chemical Society (AC-43550). Electron microscopy was acquired in the WSU Central Instrumentation Facility on a JEOL 2010 FasTEM purchased under NSF Grant DMR-0216084.

Supporting Information Available: Table of BET surface area, BJH porosity, and gel density of CdSe aerogels as a function of differing amounts of tetranitromethane; plot of SAXS data for the CdSe aerogel series. This material is available free of charge *via* the Internet at http://pubs.acs.org.

REFERENCES AND NOTES

1. Yu, H.; Li, J.; Loomis, R. A.; Wang, L.-W.; Buhro, W. E. Two-*versus* Three-Dimensional Quantum Confinement in Indium Phosphide Wires and Dots. *Nat. Mater.* **2003**, *2*, 517–520.
2. Li, L.-S.; Hu, J.; Yang, W.; Alivisatos, A. P. Band Gap Variation of Size- and Shape-Controlled Colloidal CdSe Quantum Rods. *Nano Lett.* **2001**, *1*, 349–351.
3. Mohanan, J. L.; Arachchige, I. U.; Brock, S. L. Porous Semiconductor Chalcogenide Aerogels. *Science* **2005**, *307*, 397–400.
4. Arachchige, I. U.; Brock, S. L. Sol−Gel Methods for the Assembly of Metal Chalcogenide Quantum Dots. *Acc. Chem. Res.* **2007**, *40*, 801–809.
5. Arachchige, I. U.; Mohanan, J. L.; Brock, S. L. Sol−Gel Processing of Semiconducting Metal Chalcogenide Xerogels: Influence of Dimensionality on Quantum Confinement Effects in a Nanoparticle Network. *Chem. Mater.* **2005**, *17*, 6644–6650.

6. Arachchige, I. U.; Brock, S. L. Highly Luminescent Quantum-Dot Monoliths. *J. Am. Chem. Soc.* **2007**, *129*, 1840–1841.
7. Murray, C. B.; Norris, D. J.; Bawendi, M. G. Synthesis and Characterization of Nearly Monodisperse CdE (E = S, Se, Te) Semiconductor Nanocrystallites. *J. Am. Chem. Soc.* **1993**, *115*, 8706–8715.
8. Peng, Z. A. P.; Peng, X. Formation of High-Quality CdTe, CdSe and CdS Nanocrystals Using CdO as Precursor. *J. Am. Chem. Soc.* **2001**, *123*, 183–184.
9. Murray, C. B.; Kagan, C. R.; Bawendi, M. G. Synthesis and Characterization of Mondisperse Nanocrystals and Close-Packed Nanocrystal Assemblies. *Annu. Rev. Mater. Sci.* **2000**, *30*, 545–610.
10. Arachchige, I. U.; Brock, S. L. Sol−Gel Assembly of CdSe Nanoparticles to Form Porous Aerogel Networks. *J. Am. Chem. Soc.* **2006**, *128*, 7964–7971.
11. Brock, S. L.; Arachchige, I. U.; Kalebaila, K. K. Metal Chalcogenide Gels, Xerogels and Aerogels. *Comments Inorg. Chem.* **2006**, *27*, 103–106.
12. Gacoin, T.; Malier, L.; Boilot, J.-P. New Transparent Chalcogenide Materials Using a Sol−Gel Process. *Chem. Mater.* **1997**, *9*, 1502–1504.
13. Gacoin, T.; Malier, L.; Boilot, J.-P. Sol−Gel Transition in CdS Colloids. *J. Mater. Chem.* **1997**, *7*, 859–860.
14. Pierre, A. C.; Pajonk, G. M. Chemistry of Aerogels and Their Applications. *Chem. Rev.* **2002**, *102*, 4243–4265.
15. Rolison, D. R.; Dunn, B. Electrically Conductive Oxide Aerogels: New Materials in Electrochemistry. *J. Mater. Chem.* **2001**, *11*, 963–980.
16. Yu, H.; Bellair, R.; Kannan, R. M.; Brock, S. L. Engineering Strength, Porosity, and Emission Intensity of Nanostructured CdSe Networks by Altering the Building Block Shape. *J. Am. Chem. Soc.* **2008**, *130*, 5054–5055.
17. Yu, H.; Brock, S. L. Effects of Nanoparticle Shape on the Morphology and Properties of Porous CdSe Assemblies (Aerogels). *ACS Nano* **2008**, *2*, 1563–1570.
18. Borchert, H.; Shevchenko, V. E.; Robert, A.; Mekis, I.; Kornowski, A.; Gerübel, G.; Weller, H. Determination of Nanocrystal Sizes: A Comparison of TEM, SAXS, and XRD Studies of Highly Monodisperse $CoPt_3$ Particles. *Langmuir* **2005**, *21*, 1931–1936.
19. Hüsing, N.; Schubert, U. Aerogel-Airy Materials: Chemistry, Structure, and Properties. *Angew. Chem., Int. Ed.* **1998**, *37*, 22–45.
20. Gregg, S. J.; Sing, K. S. W. *Adsorption, Surface Area and Porosity*, 2nd ed.; Academic: New York, 1982.
21. Webb, P. A.; Orr, C. *Analytical Methods in Fine Particle Technology*; Micromeritics Instrument Corp.: Norcross, GA, 1997.
22. Kagan, C. R.; Murray, C. B.; Bawendi, M. G. Long-Range Resonance Transfer of Electronic Excitations in Close-Packed CdSe Quantum-Dot Solids. *Phys. Rev. B* **1996**, *54*, 8633–8643.
23. Emmerling, A.; Fricke, J. Small Angle Scattering and the Structure of Aerogels. *J. Non-Cryst. Solids* **1992**, *145*, 113–120.
24. Dokter, W. H.; Beelen, T. P. M.; van Garderen, H. F.; van Santen, R. A.; Bras, W. Simultaneous Monitoring of Amorphous and Crystalline Phases in Silicalite Precursor Gels. An *In Situ* Hydrothermal and Time-Resolved Small- and Wide-Angle X-ray Scattering Study. *J. Appl. Crystallogr.* **1994**, *27*, 901–906.
25. Vollet, D. R.; Donatti, D. A.; Ruiz, A. I. Comparative Study Using Small-Angle X-ray Scattering and Nitrogen Adsorption in the Characterization of Silica Xerogels and Aerogels. *Phys. Rev. B* **2004**, *69*, 064202.
26. Schmidt, P. W. Small-Angle Scattering Studies of Disordered, Porous and Fractal Systems. *J. Appl. Crystallogr.* **1991**, *24*, 414–435.
27. Pająk, L.; Bierska-Piech, B.; Mrowiec-Białon, J.; Jarzębski, A. B.; Diduszko, R. SAXS from Particle and Disordered Systems. *Fibr. Text. East. Euro.* **2005**, *13*, 69–74.
28. Yu, W. W.; Qu, L.; Guo, W.; Peng, X. Experimental Determination of the Extinction Coefficient of CdTe, CdSe, and CdS Nanocrystals. *Chem. Mater.* **2003**, *15*, 2854–2860.
29. Mohanan, J. L.; Brock, S. L. A New Addition to the Aerogel Community: Unsupported CdS Aerogels with Tunable Optical Properties. *J. Non-Cryst. Solids* **2004**, *350*, 1–8.
30. Wendlandt, W. W.; Helcht, H. G. *Chemical Analysis: Reflectance Spectroscopy*; Interscience: New York, 1966; Vol. 21.
31. Tandon, S. P.; Gupta, J. P. Measurement of Forbidden Energy Gap of Semiconductors by Diffuse Reflectance Technique. *Phys. Status Solidi* **1970**, *38*, 363–367.
32. Ito, Y.; Omote, K.; Harada, H., A New Small Angle X-ray Scattering Technique for Determining Nano-Scale Pore/Particle Size Distributions in Thin Film. In *Advances in X-ray Analysis*; JCPDS-International Center for Diffraction Data: 2003; Vol. 46, pp 56−60.
33. Sasaki, A. Size Distribution Analysis of Nanoparticles Using Small Angle X-ray Scattering Technique. *Rigaku J.* **2005**, *22*, 31–38.